Evaluation of Exchange-Correlation Functionals for Time-Dependent Density Functional Theory Calculations on Metal Complexes

ARTICLE *in* JOURNAL OF COMPUTATIONAL CHEMISTRY · JANUARY 2009

Impact Factor: 3.59 · DOI: 10.1002/jcc.21385 · Source: PubMed

2 AUTHORS:

Jason P Holland
Harvard Medical School
66 PUBLICATIONS **1,482** CITATIONS
SEE PROFILE

Jennifer C Green
University of Oxford
393 PUBLICATIONS **8,758** CITATIONS
SEE PROFILE

Evaluation of Exchange-Correlation Functionals for Time-Dependent Density Functional Theory Calculations on Metal Complexes

JASON P. HOLLAND,* JENNIFER C. GREEN
Department of Chemistry, Chemistry Research Laboratory, University of Oxford, 12 Mansfield Road, Oxford OX1 3TA, United Kingdom

Received 7 May 2009; Accepted 2 July 2009
DOI 10.1002/jcc.21385
Published online 23 September 2009 in Wiley InterScience (www.interscience.wiley.com).

Abstract: The electronic absorption spectra of a range of copper and zinc complexes have been simulated by using time-dependent density functional theory (TD-DFT) calculations implemented in Gaussian03. In total, 41 exchange-correlation (XC) functionals including first-, second-, and third-generation (meta-generalized gradient approximation) DFT methods were compared in their ability to predict the experimental electronic absorption spectra. Both pure and hybrid DFT methods were tested and differences between restricted and unrestricted calculations were also investigated by comparison of analogous neutral zinc(II) and copper(II) complexes. TD-DFT calculated spectra were optimized with respect to the experimental electronic absorption spectra by use of a Matlab script. Direct comparison of the performance of each XC functional was achieved both qualitatively and quantitatively by comparison of optimized half-band widths, root-mean-squared errors (RMSE), energy scaling factors (ε_{SF}), and overall quality-of-fit (Q_F) parameters. Hybrid DFT methods were found to outperform all pure DFT functionals with B1LYP, B97-2, B97-1, X3LYP, and B98 functionals providing the highest quantitative and qualitative accuracy in both restricted and unrestricted systems. Of the functionals tested, B1LYP gave the most accurate results with both average RMSE and overall $Q_F < 3.5\%$ and ε_{SF} values close to unity (>0.990) for the copper complexes. The XC functional performance in spin-restricted TD-DFT calculations on the zinc complexes was found to be slightly worse. PBE1PBE, mPW1PW91 and B1LYP gave the most accurate results with typical RMSE and Q_F values between 5.3 and 7.3%, and ε_{SF} around 0.930. These studies illustrate the power of modern TD-DFT calculations for exploring excited state transitions of metal complexes.

 J Comput Chem 31: 1008–1014, 2010

Key words: time-dependent density functional theory; exchange-correlation; electronic absorption spectroscopy; excited states; copper

Introduction

Over the last few decades, density functional theory[1,2] (DFT) has affirmed its place as an important tool for use in modern chemical analysis of organic and inorganic systems. Calculation of physical properties such as geometries, normal modes of vibration, ionization potentials, reaction thermodynamics, and kinetic barrier heights with chemical accuracy and low computational expense remains the cornerstone of computational chemistry. Other properties of particular interest to transition metal coordination chemists include redox potentials, NMR chemical shifts, electron paramagnetic resonance coupling constants, and calculation of excited state transitions for prediction of electron absorption spectra.[3–10]

Problems associated with the calculation of excited states using both density and wave functions based methods are well documented.[3] Several strategies have been proposed to extract excited state information from the ground state density; the most promising of which is time-dependent (TD)-DFT devised by Runge and Gross.[3,11] The theoretical foundation and application of TD-DFT calculations have been the subject of several excellent reviews.[12–20]

From a practical standpoint, TD-DFT calculates the frequency-dependent linear response of the charge density with respect to a time-dependent perturbation in the electric field.[3,13]

Additional Supporting Information may be found in the online version of this article.

*Present address: Department of Radiology, Memorial Sloan-Kettering Cancer Center, 1275 York Avenue, New York, New York 10065.

Correspondence to: J.P. Holland; e-mail: hollanj3@mskcc.org or jasonpholland@gmail.com

Contract/grant sponsor: Engineering and Physical Sciences Research Council (EPSRC) and Merton College

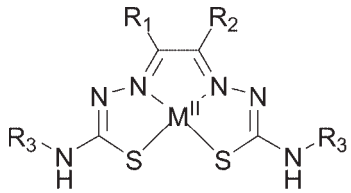

Complex	R_1	R_2	R_3
1 [Cu^{II}ATSM]	Me	Me	Me
2 [Zn^{II}ATSM]	Me	Me	Me
3 [Cu^{II}GTS]	H	H	H
4 [Cu^{II}PTS]	Me	H	H

Figure 1. Structures of the copper and zinc *bis*(thiosemicarbazonato) complexes used for TD-DFT functional testing. The syntheses and characterization of complexes **1–4** have been reported elsewhere.[29–33]

The results include calculation of excitation energies ω_I and oscillator strengths f_I for transition between the ground and excited states I of a system.[21] This elegant solution circumvents the difficulties associated with the calculation of excited states by describing these excitations in terms of ground state properties such as molecular orbital (MO) contributions.

Several groups have compared the quantitative accuracy of TD-DFT calculations.[22–24] For exchange-correlation (XC) functionals utilizing the generalized gradient approximation[25,26] (GGA), typical errors in calculated ω_I values are reported to be on the order of a few tenths of an electron volt (eV).[23,24] Due to the dependence on solvation, larger variations are to be expected between experimental and calculated values of f_I. However, as noted by Boese and Handy[27] and Zhao et al.[28] studies on the performance of different XC functionals for the calculation of physical properties beyond standard benchmark tests are comparatively rare. End users of commercially available computational software often base their choice of XC functional on popularity rather than performance. Such attitudes have been beneficial in that the use of DFT has become the mainstream, particularly in inorganic chemistry, but they have also limited the adoption of more accurate second- and third-generation functionals.

The focus of the present work is on the calculation of transition metal complexes for which experimental characterization by photoelectron spectroscopy, electronic absorption spectroscopy (UV/vis), and spectroelectrochemistry often provides revealing information about molecular structure. This article compares the performance of 41 different XC functionals in their ability to predict the UV/vis spectra of copper and zinc *bis*(thiosemicarbazonato) complexes (see Fig. 1).[29–33] These complexes are of particular interest in our continuing efforts towards developing copper complexes for *in vivo* positron emission tomography imaging of hypoxic tumors (tissue oxygenation levels pO_2 <3 mmHg).

Computational Details

All the calculations reported were conducted by using either restricted (for singlet state [Zn^{II}ATSM]) or unrestricted (for doublet state copper complexes) methods implemented in Gaussian03 (Revision D.01).[34] Normal self-consistent field (SCF) and geometry convergence criteria were used and no symmetry constraints were imposed. All structures were optimized by using the 6–311++G(d,p) basis set for all atoms[35,36] (please refer to the supporting information). This double-ζ basis set has been shown to provide an excellent balance between computational accuracy and expense, and is generally affordable by most computational users for medium-sized systems (400–600 basis functions). For the largest complexes studied, [Cu^{II}ATSM] and [Zn^{II}ATSM], a total of 445 basis functions were used. Harmonic frequency calculations based on analytical second derivatives were used to characterize the optimized geometries as local minima. The effect of solvation was also investigated by performing the TD-DFT calculations in the presence of a self-consistent reaction field (SCRF) by using the integral equation formalism polarizable comntinuum models (IEFPCM) with varying values of the dielectric constant (ε = 10–80) and solvent probe sphere radius (R_{solv} = 1.0–5.0 Å).[37–40] The solute–solvent boundary was defined by using solvent excluding surface[41] combined with the United Atom Hartree-Fock topological model for the radii of the solute atoms.[42] Structures were reoptimized in the presence of the SCRF before performing the TD-DFT calculations. Although the physical interpretation of TD-DFT calculations performed in the presence of a polarizable continuum solvation model is questionable, these calculations have been performed for comparison, and the results should be treated with caution.

The 41 XC functionals investigated can be divided into four categories: (i) pure GGA functionals (where X = 0) including the first-generation BLYP,[43,44] BP86,[10,44,45] BPW91,[44,46,47] PW91PW91,[46,47] and second-generation methods; BPBE,[25,44] PBEPBE,[25] PBEP86,[10,25,26,45] PBELYP,[25,43] PBE1W[48] (invoked with the PBEPBE and Iop[3/78 = 0740010000] keywords), BV5LYP,[43,49] OLYP,[43,50,51] OP86,[10,45,50,51] OPW91,[46,47,50] G96LYP,[43,52] and mPWPW91[46,53]; (ii) hybrid GGA functionals (where X > 0) including the first-generation B1LYP,[43,44,54] B3LYP,[43,44,55] B3P86,[10,44,45] B3PW91,[44,46,56] BHandH[34,57] and second-generation methods B97-1,[58,59] B97-2,[58–60] B98,[58,61] O3LYP,[43,50,51] X3LYP[43,62] PBE1PBE (also known as PBE0),[25,26,63] THCTHH,[27] mPW1PW91,[46,53,64] mPW3LYP (mPWLYP combined with Iop(3/76 = 1000002000), Iop(3/77 = 0720008000) and (Iop[3/78 = 0810010000] keywords),[65] MPW1N (mPWPW91 and Iop[3/76 = 0594004060]),[64,66] MPW1K (mPWPW91 and Iop[3/76 = 0572004280]),[64,67] and MPW1S (mPWPW91 and Iop[3/76 = 0940000600])[64]; (iii) pure meta-GGA functionals including BB95,[44,68] BTPSS,[44,69] TPSSTPSS,[69] VSXC,[70] and MPWB1K (mPWB95 and Iop[3/76 = 0560004400])[53,65,68]; (iv) hybrid meta-GGAs including BB1K (BB95 and Iop[3/76 = 0580004200]),[44,68,71] TPSSh,[72] TPSS1KCIS[69,73,74] (TPSSKCIS and Iop[3/76 = 0870001300]) and BMK.[75] The origins and nomenclature of the XC functionals studied have been described elsewhere.[28,76]

Results and Discussion

Time-dependent density functional theory calculations were conducted using input geometries of complexes **1–4** optimized at

the same level of theory. In each case, oscillator strengths and excitation energies for transition between the ground state and the first 24 excited stated states were calculated. In previous work,[30,31,33] we used the SWizard program[77] by Gorelsky to produce simulated UV/vis spectra based on the TD-DFT calculations. Each calculated transition between the ground and excited states I, can be modeled by, for example, a single Gaussian function in accordance with eq. (1).

$$\varepsilon(\omega) = 2.174 \times 10^8 \sum_I \frac{f_I}{\Delta_{1/2,I}} \exp\left(-2.773 \frac{(\omega - \omega_I)^2}{\Delta_{1/2,I}^2}\right) \quad (1)$$

$$\sum_I f_I = 4.319 \times 10^{-9} \int \varepsilon(\omega) d\omega \quad (2)$$

Modeled parameters include the molar absorption coefficient ε (dimensionless), TD-DFT calculated excitation energies, ω_I (in cm^{-1}), transition oscillator strength, f_I (dimensionless), and half-band width, $\Delta_{1/2,I}$ (in cm^{-1}). The total integrated intensity under the absorption profile is equal to the sum of the oscillator strengths and is given by eq. (2).

For low resolution spectroscopy, Gaussian functions have been shown to be suitable for accurate simulation of experimental band shapes.[78] Experimental half-band widths are generally unknown, and are difficult to estimate due to their high dependence on solvation and/or vibronic coupling within the system. Previous studies have used a single global value of $\Delta_{1/2}$ applied to each transition with nonzero f_I values to generate the simulated spectra.[30,31] However, this arbitrary choice of $\Delta_{1/2}$ prevents accurate comparison of the relative and absolute performance of each XC functional.

To facilitate direct comparison of the performance of each XC functional, we used Matlab to apply Gaussian functions with variable $\Delta_{1/2,I}$ to each calculated transition, and minimized the variance between the experimental and simulated UV/vis spectra. Calculated energies are often scaled, particularly in vibrational frequency analysis.[3] Therefore, an energy scaling factor, ε_{SF}, was also optimized for each calculation. Finally, after minimization, the root-mean-squared error (RMSE/%) and quality of fit (Q_F/%) were calculated for each simulated spectrum.

The optimized fit parameters between the experimental and calculated TD-DFT spectra for complexes **1** and **2** are presented in Table 1. The syntheses and characterization of complex **1–4** have been reported elsewhere.[30,31,33] The optimized geometries have also been compared to three experimental X-ray crystal structures and the root-mean-squared deviation (RMSD/Å) values are presented.[79,80] The results show that in almost all cases hybrid DFT functionals outperform pure functionals in both restricted and unrestricted TD-DFT calculations. For copper complexes **1**, **3,** and **4** (Tables 1 and 2), B1LYP gave the best quantitative results with Q_F values of 3.74, 3.87, and 3.14%, respectively, and ε_{SF} values close to unity (>0.99). In these studies, ε_{SF} values less than unity indicate that the calculations underestimate the experimental excitation energies. An overlay plot of the experimental UV/vis spectrum of complex **1** (0.05 mM in dimethyl formamide at 298 K) and the TD-DFT simulated spectrum using the B1LYP method is shown in Figure 2.[30,33] Qualitatively, the B1LYP simulated spectrum reproduces all spectral features (peaks, shoulders, and troughs) observed in the experimental UV/vis spectrum with high accuracy.

Other hybrid functionals which perform well and gave both quantitative and qualitatively accurate results include B97-2, B97-1, X3LYP, and B98. The popular B3LYP functional also provides a satisfactory fit (Q_F = 6.42% and ε_{SF} = 0.975), and is ranked second amongst first-generation methods (behind B1LYP) but is less accurate than most second-generation hybrid functionals tested (ranked ninth overall).

The meta-GGA VSXC method gave the best performance of all pure DFT functionals with Q_F = 7.44%. For VSXC, the main spectral features were reproduced but errors were found to occur in both high and low energy regions of the spectrum. This is a general characteristic observed in the simulated spectra of all pure functionals tested which indicates that these XC functionals provide poor estimates of both occupied and virtual MO energies, despite giving reasonably accurate calculated structures (based on weighted RMSD values).

The pure and hybrid meta-GGA functionals gave better performance than pure first- and second-generation DFT methods. For complex **1**, TPSS1KCIS gave the best results with Q_F = 7.89%, and is ranked 13th overall behind most second-generation hybrid GGA methods. Hybrid versions of meta-GGA functionals (BB1K) also perform better than their pure DFT counterparts (BB95), but the overall improvement in simulated spectra is negligible.

Hybrid functionals with Hartree-Fock percentages (%HF) >30%, were found to reduce the quality of the simulated TD-DFT spectra. This is perhaps not unexpected as the functionals tested (MPW1N, MPW1K, BMK, and BB1K) were originally optimized for the calculation of kinetic barrier heights and not for overall performance in wider benchmark tests.[28] If these functionals are excluded, linear regression analysis between the Q_F values and %HF calculated for complexes **1** and **2** give R^2-values of 0.79 and 0.77, respectively. These data demonstrates the somewhat weak but important dependence of the calculated ω_I and f_I values on the %HF mixed into the hybrid DFT functionals.

The effect of increasing the basis set size was also investigated by calculating the TD-DFT simulated spectrum of **1** using the uB3LYP/6–311++G(d,p) methodology (Table 1). TD-DFT calculations have been reported to be relatively insensitive to changes in basis set size,[3,24] and the optimized Q_F value of 6.07% represents only a 0.35% improvement over the calculation using the double-ζ basis set.

It was found that for both copper and zinc complexes, XC functionals which gave Q_F values >8.0% failed to reproduce all experimentally observed spectral features with most of the error associated with inaccurate calculation of the low energy transitions.

Again, for restricted TD-DFT calculations on the zinc complex **2**, hybrid DFT functionals were found to outperform pure functionals. Errors were larger, with only three XC functionals giving Q_F values <8.0%. PBE1PBE, mPW1PW91, and B1LYP

Table 1. Comparison of Different XC Functionals in the TD-DFT Calculations on Complexes **1** and **2**.

		[Cu^{II}ATSM] (**1**)[a]						[Zn^{II}ATSM] (**2**)[b]			
XC[c]	%HF	RMSD[d] (Å)	RMSD[e] (Å)	RMSD[f] (Å)	RMSE (%)	ε_{SF}	Q_F (%)[g]	RMSE (%)	ε_{SF}	Q_F (%)	Rank
B1LYP	25	0.0477	0.0643	0.0709	3.73	0.996	3.74	6.85	0.934	7.34	3
B97-2	21	0.0345	0.0566	0.0621	4.90	0.999	4.90	8.12	0.920	8.83	4
B97-1	21	0.0429	0.0610	0.0677	5.99	0.997	6.01	8.77	0.910	9.64	7
X3LYP	21.8	0.0444	0.0621	0.0685	6.13	0.993	6.17	9.02	0.910	9.92	9
B98	21.98	0.0418	0.0604	0.0670	6.18	1.000	6.18	8.93	0.920	9.71	8
mPW3LYP	20	0.0451	0.0626	0.0690	6.14	0.987	6.22	9.61	0.900	10.68	11
THCTHH	15	0.0350	0.0564	0.0628	5.19	0.810	6.40	11.03	0.877	12.58	12
B3LYP	20	0.0457	0.0630	0.0696	6.26	0.975	6.42	9.56	0.900	10.63	10
O3LYP	11.61	0.0382	0.0587	0.0654	5.80	0.792	7.32	12.00	0.860	13.96	17
B3P86	20	0.0280	0.0534	0.0582	7.16	1.027[h]	7.36	8.53	0.900	9.47	6
mPW1PW91	25	0.0290	0.0539	0.0586	6.68	0.891	7.49	5.81	0.930	6.25	2
PBE1PBE	25	0.0287	0.0538	0.0583	6.76	0.900	7.51	5.33	0.933	5.72	1
TPSS1KCIS	13	0.0351	0.0565	0.0625	6.45	0.817	7.89	11.09	0.880	12.60	13
B3PW91	20	0.0299	0.0541	0.0596	7.88	0.998	7.90	8.47	0.900	9.41	5
MPW1N	40.6	0.0336	0.0569	0.0601	7.94	0.970	8.19	17.30	1.000	17.30	38
BMK	42	0.0438	0.0675	0.0618	8.18	1.016	7.32	16.86	1.000	16.86	37
VSXC	0	0.0662	0.0793	0.0835	7.44	0.893	8.33	14.31	0.818	17.50	35
MPW1K	42.8	0.0349	0.0577	0.0606	8.50	0.992	8.57	19.21	1.000	19.21	40
TPSSh	10	0.0317	0.0547	0.0606	7.26	0.814	8.91	11.86	0.871	13.62	15
MPWB1K	0	0.0372	0.0594	0.0613	8.40	0.930	9.03	17.78	1.000	17.78	39
OLYP	0	0.0461	0.0636	0.0711	7.22	0.748	9.65	12.18	0.970	12.55	19
BB1K	42	0.0354	0.0582	0.0605	9.22	0.910	10.13	16.14	1.000	16.14	36
MPW1S	6	0.0341	0.0560	0.0625	8.16	0.767	10.64	12.63	0.820	15.40	21
OP86	0	0.0283	0.0542	0.0600	9.20	0.845	10.89	12.77	0.800	15.97	22
PW91PW91	0	0.0356	0.0567	0.0634	9.26	0.830	11.15	13.13	0.776	16.91	27
BLYP	0	0.0659	0.0776	0.0854	8.29	0.732	11.33	11.91	0.940	12.67	16
TPSSTPSS	0	0.0362	0.0570	0.0637	8.91	0.777	11.47	13.08	0.808	16.19	24
PBEP86	0	0.0390	0.0585	0.0654	9.59	0.823	11.65	13.33	0.762	17.50	31
PBE1W	0	0.0475	0.0640	0.0713	9.45	0.807	11.71	11.38	0.970	11.73	14
PBEPBE	0	0.0368	0.0574	0.0642	9.67	0.824	11.74	13.09	0.771	16.98	25
BP86	0	0.0400	0.0593	0.0665	9.67	0.823	11.75	12.16	0.960	12.67	18
BV5LYP	0	0.0659	0.0776	0.0854	9.31	0.789	11.80	13.78	0.760	18.14	34
PBELYP	0	0.0652	0.0770	0.0845	8.66	0.731	11.84	13.29	0.970	13.70	30
mPWPW91	0	0.0380	0.0581	0.0651	9.74	0.820	11.88	13.48	0.780	17.28	33
OPW91	0	0.0286	0.0545	0.0603	9.13	0.768	11.89	12.51	0.808	15.49	20
G96LYP	0	0.0579	0.0716	0.0794	8.86	0.739	11.99	13.45	0.940	14.31	32
BB95	0	0.0381	0.0580	0.0647	9.57	0.798	12.00	13.18	0.760	17.35	29
BPBE	0	0.0379	0.0582	0.0653	10.09	0.759	13.29	13.03	0.780	16.71	23
BPW91	0	0.0395	0.0590	0.0662	10.07	0.756	13.32	13.11	0.780	16.81	26
BTPSS	0	0.0396	0.0591	0.0664	10.07	0.752	13.39	13.17	0.780	16.88	28
BHandH	50	0.0448	0.0652	0.0650	15.29	0.726	21.06	–	–	–	–
B3LYP/6–311++G(d,p)[i]	20	0.0444	0.0617	0.0683	5.94	0.978	6.07	–	–	–	–

[a]Unrestricted calculations.
[b]Restricted calculations.
[c]Listed in the order of the lowest calculated value of Q_F for complex **1**.
[d]Weighted root-mean-squared deviation (RMSD) between the DFT optimized geometries and the experimental X-ray crystal structures with Cambridge Crystallographic Database Codes, CCDC: XOBNIL.
[e]UMUXUV (dimethyl sulphoxide omitted).
[f]UMUYAC (dimethyl formamide omitted).
[g]Q_F = RMSE/ε_{SF}.
[h]For the calculation of Q_F this energy scaling factor is equivalent to 0.973.
[i]TD-DFT calculation performed by using the larger triple-ζ basis set 6–311++G(d,p).

gave the best results with Q_F values of 5.72, 6.25, and 7.34%, respectively. Figure 3 shows an overlay plot of the experimental UV/vis spectrum of complex **2** (0.05 mM in dimethyl formamide at 298 K) and the TD-DFT simulated spectra calculated by using the PBE1PBE and B3LYP methods. In comparison to the TD-DFT calculations on the copper complexes, the optimized ε_{SF}

Table 2. Time-Dependent Density Functional Theory Optimised Fit Parameters for Copper Complexes **3** and **4**.

	[Cu^{II}GTS] (**3**)			[Cu^{II}PTS] (**4**)		
XC[a]	RMSE (%)	ε_{SF}	Q_F (%)	RMSE (%)	ε_{SF}	Q_F (%)
B1LYP	3.83	0.99	3.87	3.10	0.99	3.14
B98	5.87	1.00	5.87	3.98	1.00	3.98
X3LYP	6.54	0.99	6.60	6.32	0.99	6.38
B3LYP	6.62	0.98	6.75	4.99	0.98	5.10
TPSSh	6.18	0.83	7.44	6.85	0.83	8.25
O3LYP	6.63	0.80	8.29	6.21	0.81	7.67
MPW1K	8.24	0.91	9.05	–	–	–
PBE1PBE	8.51	0.92	9.25	7.48	0.91	8.22
MPW1N	8.91	0.91	9.79	–	–	–
mPW1PW91	9.31	0.92	10.12	–	–	–
B97-2	8.87	0.85	10.44	5.56	1.00	5.56
OP86	8.53	0.77	11.07	–	–	–
BLYP	8.24	0.73	11.28	8.33	0.74	11.24
BV5LYP	8.24	0.73	11.28	–	–	–
B97-1	9.64	0.85	11.34	5.17	1.00	5.17
VSXC	8.66	0.76	11.39	7.94	0.90	8.82
mPW3LYP	10.08	0.88	11.46	–	–	–
MPWB1K	10.08	0.88	11.46	–	–	–
PBELYP	8.38	0.73	11.48	8.39	0.75	11.19
PW91PW91	9.16	0.76	12.05	–	–	–
B3PW91	10.26	0.85	12.07	8.35	0.86	9.71
B3P86	10.27	0.85	12.08	8.57	0.86	9.97
BB1K	11.72	0.97	12.09	–	–	–
PBEPBE	9.07	0.75	12.10	9.10	0.79	11.52
BTPSS	9.21	0.76	12.11	–	–	–
PBE1W	9.19	0.74	12.42	–	–	–
BPW91	9.48	0.76	12.48	–	–	–
OLYP	9.28	0.74	12.54	8.97	0.74	12.12
BVP86	9.58	0.76	12.60	–	–	–
G96LYP	9.58	0.76	12.60	–	–	–
BB95	11.18	0.81	13.81	–	–	–
BHandH	16.76	1.00	16.76	–	–	–

[a]Listed in the order of the lowest calculated value of Q_F for complex **3**.

values were considerably lower, typically around 0.900–0.934 for the best performing methods. These data indicate that for complex **2** the restricted TD-DFT calculations are only able to reproduce the excited state transition energies to within ~90% of the true values. The best performing method, PBE1PBE still gave a low ε_{SF} value of 0.934 which suggests that the calculated electronic structure of **2** is not a very accurate description of the real system observed in the UV/vis experiment. This error may be a problem with the computation but is more likely due to the fact that zinc(II) *bis*(thiosemicarbazonato) complexes are known to bind a fifth donor atom (such as solvent molecules including dimethyl formamide and dimethyl sulphoxide) in the apical site.[81] The pseudo square-planar structure of complex **2** used in these calculations is not fully representative of the experiment. Attempts to model the coordination of a solvent molecule to the axial coordination site of complex **2** did not improve the results of the TD-DFT calculations.

Inclusion of solvation effects in the TD-DFT calculations on complex **1** using the B1LYP and B3LYP XC functionals was found to have negligible effect on the calculated values of ω_I and f_I. When the IEFPCM dielectric constant was varied the calculated values of ω_I were found to shift to higher energy by an average of between 3 and 5 nm on moving from ε = 10.0 to 80.0 with R_{solv} = 2.0 Å. Variations in solvent probe sphere radius were also found to have a negligible effect on the calculated excitation energies with values of ω_I shifting to lower energy by an average of 4 nm for an increase in R_{solv} between 1.0 and 5.0 Å, at ε = 40.0. These observed changes in ω_I are in line with the expected energy stabilization of the ground state MOs with increasing values of ε, and decreased MO stabilization with increasing R_{solv} (due to decreased solvent–solute contact). Overall, the inclusion of solvation effects did not improve the quality of either the B1LYP or B3LYP TD-DFT calculations.

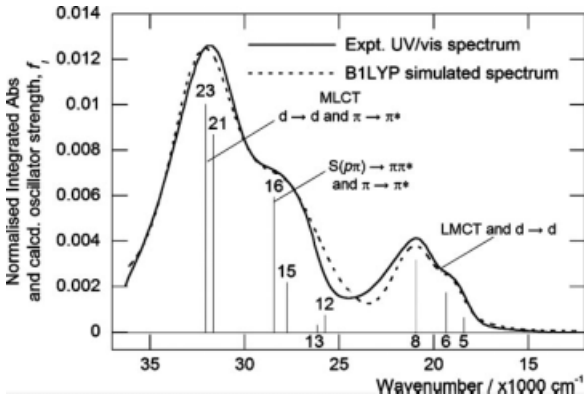

Figure 2. Overlay of the experimental UV/vis spectrum (solid) of complex **1** and TD-DFT simulated spectrum (dashed) calculated by using the B1LYP XC functional. Vertical bars correspond to transitions between the ground and excited states I with nonzero calculated oscillator strengths (numbered inset) (RMSE = 3.73%, ε_{SF} = 0.996, and Q_F = 3.74%).

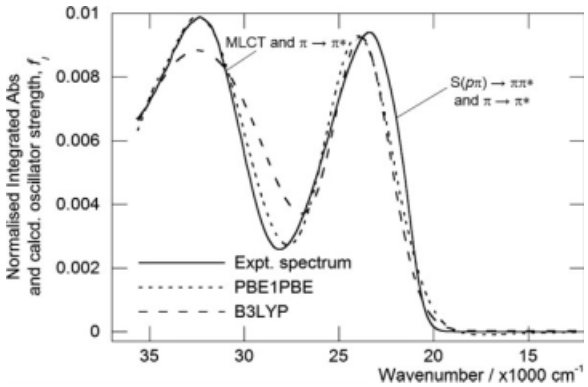

Figure 3. Overlay of the experimental UV/vis spectrum of complex **2** and TD-DFT simulated spectra calculated by using the PBE1PBE and B3LYP XC functionals. In comparison to the best performing functional (PBE1PBE, Q_F = 5.72%) both the qualitative and quantitative accuracy of the B3LYP functional (Q_F = 10.63%) are reduced due to inaccurate calculation of higher energy excited state transitions.

Summary and Conclusions

The relative and absolute performance of a wide range of XC functionals has been evaluated for use in TD-DFT calculations of UV/vis spectra of transition metal complexes. The results indicate that hybrid functionals provide the best description of the electronic excited state transitions (both ω_I and f_I values) but larger variations are observed depending on the system studied. B1LYP, B97-2, and B97-1 gave consistently high performance irrespective of the electronic configuration (closed or open shell) and structure. With judicious selection of the calculation method and appropriate functional testing, TD-DFT calculations have the potential to provide highly accurate predictions of electronic absorption spectra for transition metal complexes and are set to play an ever increasing role in the analysis of complex systems. Further studies investigating TD-DFT calculations on a broader range of metal complexes with varying metals, oxidations states, and coordination geometries are underway. These findings may also help to stimulate the development of new functionals designed specifically for use in TD-DFT calculations.

Acknowledgments

The authors thank Dr Martin Bell for assistance with Matlab and the Oxford Supercomputing Centre (OSC).

References

1. Hohenberg, P.; Kohn, W. Phys Rev B 1964, 136, 864.
2. Kohn, W.; Sham, L. J Phys Rev A 1965, 140, 1133.
3. Koch, W.; Holthausen, M. C. A Chemist's Guide to Density Functional Theory, 2nd ed., Wiley-VCH, Weinheim, Germany, 2001.
4. Parr, R. G.; Yang, W. Density-Functional Theory of Atoms and Molecules, Oxford University Press, New York, 1989.
5. Kohn, W.; Becke, A. D.; Parr, R. G. J Phys Chem 1996, 100, 12974.
6. Nagy, A. Phys Reports 1998, 298, 1.
7. Baerends, E. J.; Gritsenko, O. V. J Phys Chem A 1997, 101, 5383.
8. Geerlings, P.; De Proft, F.; Langenaeker, W. Chem Rev 2003, 103, 1793.
9. Perdew, J. P. NATO ASI Series B: Phys 1985, 123, 265.
10. Perdew, J. P. Phys Rev B 1986, 33, 8800.
11. Runge, E.; Gross, E. K. U. Phys Rev Lett 1984, 52, 997.
12. Theophilou, A. K. J Phys C 1979, 12, 5419.
13. Gross, E. K. U.; Kohn, W. Adv Quantum Chem 1990, 21, 255.
14. Petersilka, M.; Gossmann, U. J.; Gross, E. K. U. Phys Rev Lett 1996, 76, 1212.
15. Nagy, A. Phys Rev A 1998, 57, 1672.
16. Nagy, A. Int J Quantum Chem 1998, 70, 681.
17. Casida, M. E. Recent Adv Comp Chem 1995, 1, 155.
18. Burke, K.; Gross, E. K. U. Lecture Notes in Phys 1998, 500, 116.
19. Burke, K.; Werschnik, J.; Gross, E. K. U. J Chem Phys 2005, 123, 062206/062201.
20. Marques, M. A. L.; Gross, E. K. U. Ann Rev Phys Chem 2004, 55, 427.
21. Ullrich, C. A. J Chem Theory Comp 2009, 5, 859.
22. Jacquemin, D.; Perpete, E. A.; Scuseria, G. E.; Ciofini, I.; Adamo, C. Chem Phys Lett 2008, 465, 226.
23. Casida, M. E.; Casida, K. C.; Salahub, D. R. Int J Quantum Chem 1998, 70, 933.
24. Stratmann, R. E.; Scuseria, G. E.; Frisch, M. J. J Chem Phys 1998, 109, 8218.
25. Perdew, J. P.; Burke, K.; Ernzerhof, M. Phys Rev Lett 1996, 77, 3865.
26. Perdew, J. P.; Burke, K.; Wang, Y. Phys Rev B 1996, 54, 16533.
27. Boese, A. D.; Handy, N. C. J Chem Phys 2002, 116, 9559.
28. Zhao, Y.; Pu, J.; Lynch, B. J.; Truhlar, D. G. Phys Chem Chem Phys 2004, 6, 673.
29. Holland, J. P.; Green, J. C.; Dilworth, J. R. Dalton Trans 2006, 6, 783.
30. Holland, J. P.; Aigbirhio, F. I.; Betts, H. M.; Bonnitcha, P. D.; Burke, P.; Christlieb, M.; Churchill, G. C.; Cowley, A. R.; Dilworth, J. R.; Donnelly, P. S.; Green, J. C.; Peach, J. M.; Vasudevan, S. R.; Warren, J. E. Inorg Chem 2007, 46, 465.
31. Holland, J. P.; Barnard, P. J.; Bayly, S. R.; Betts, H. M.; Churchill, G. C.; Dilworth, J. R.; Edge, R.; Green, J. C.; Hueting, R. Eur J Inorg Chem 2008, 12, 1985.
32. Holland, J. P.; Barnard, P. J.; Collison, D.; Dilworth, J. R.; Edge, R.; Green, J. C.; Heslop, J. M.; McInnes, E. J. L.; Salzmann, C. G.; Thompson, A. L. Eur J Inorg Chem 2008, 22, 3549.
33. Holland, J. P.; Barnard, P. J.; Collison, D.; Dilworth, J. R.; Edge, R.; Green, J. C.; McInnes, E. J. L. Chem A Eur J 2008, 14, 5890.
34. Frisch, M. J.; Trucks, G. W.; Schlegel, H. B.; Scuseria, G. E.; Robb, M. A.; Cheeseman, J. R.; Montgomery, J. A., Jr; Vreven, T.; Kudin, K. N.; Burant, J. C.; Millam, J. M.; Iyengar, S. S.; Tomasi, J.; Barone, V.; Mennucci, B.; Cossi, M.; Scalmani, G.; Rega, N.; Petersson, G. A.; Nakatsuji, H.; Hada, M.; Ehara, M.; Toyota, K.; Fukuda, R.; Hasegawa, J.; Ishida, M.; Nakajima, T.; Honda, Y.; Kitao, O.; Nakai, H.; Klene, M.; Li, X.; Knox, J. E.; Hratchian, H. P.; Cross, J. B.; Bakken, V.; Adamo, C.; Jaramillo, J.; Gomperts, R.; Stratmann, R. E.; Yazyev, O.; Austin, A. J.; Cammi, R.; Pomelli, C.; Ochterski, J. W.; Ayala, P. Y.; Morokuma, K.; Voth, G. A.; Salvador, P.; Dannenberg, J. J.; Zakrzewski, V. G.; Dapprich, S.; Daniels, A. D.; Strain, M. C.; Farkas, O.; Malick, D. K.; Rabuck, A. D.; Raghavachari, K.; Foresman, J. B.; Ortiz, J. V.; Cui, Q.; Baboul, A. G.; Clifford, S.; Cioslowski, J.; Stefanov, B. B.; Liu, G.; Liashenko, A.; Piskorz, P.; Komaromi, I.; Martin, R. L.; Fox, D. J.; Keith, T.; Al-Laham, M. A.; Peng, C. Y.; Nanayakkara, A.; Challacombe, M.; Gill, P. M. W.; Johnson, B.; Chen, W.; Wong, M. W.; Gonzalez, C.; Pople, J. A. Gaussian 03; Gaussian Inc.: Wallingford, CT, 2004.
35. Rassolov, V. A.; Pople, J. A.; Ratner, M. A.; Windus, T. L. J Chem Phys 1998, 109, 1223.
36. Rassolov, V. A.; Ratner, M.; Pople, J. A.; Redfern, P. C.; Curtiss, L. A. J Comp Chem 2001, 22, 976.
37. Hall, R. J.; Davidson, M. M.; Burton, N. A.; Hillier, I. H. J Phys Chem 1995, 99, 921.
38. Chen, J. L.; Noodleman, L.; Case, D. A.; Bashford, D. J Phys Chem 1994, 98, 11059.
39. Tomasi, J.; Mennucci, B.; Cances, E. Theochem 1999, 464, 211.
40. Tomasi, J.; Mennucci, B.; Cammi, R. Chem Rev 2005, 105, 2999.
41. Connolly, M. L. Science 1983, 221, 709.
42. Barone, V.; Cossi, M.; Tomasi, J. J Chem Phys 1997, 107, 3210.
43. Lee, C.; Yang, W.; Parr, R. G. Phys Rev B 1988, 37, 785.
44. Becke, A. D. Phys Rev A 1988, 38, 3098.
45. Perdew, J. P. Phys Rev B 1986, 33, 8822.
46. Perdew, J. P. Electronic Structure of Solids '91, Akademie Verlag, Berlin, Germany, 1991; pp. 11.
47. Burke, K.; Perdew, J. P.; Wang, Y. Derivation of a generalized gradient approximation: the PW91 density functional. Electron Density Functional Theory: Recent Progress and New Directions, [Proceedings of the International Workshop on Electronic Density Functional Theory: Recent Progress and New Directions], Nathan, Australia, July 14-19, 1996 (1998), Meeting Date 1996, 1998; pp. 81.
48. Dahlke, E. E.; Truhlar, D. G. J Phys Chem B 2005, 109, 15677.
49. Vosko, S. H.; Wilk, L.; Nusair, M. Can J Phys 1980, 58, 1200.
50. Handy, N. C.; Cohen, A. J Mol Phys 2001, 99, 403.
51. Hoe, W. M.; Cohen, A. J.; Handy, N. C. Chem Phys Lett 2001, 341, 319.
52. Gill, P. M. W. Mol Phys 1996, 89, 433.

53. Adamo, C.; Barone, V. J Chem Phys 1998, 108, 664.
54. Adamo, C.; Barone, V. Chem Phys Lett 1997, 274, 242.
55. Stephens, P. J.; Devlin, F. J.; Chabalowski, C. F.; Frisch, M. J. J Phys Chem 1994, 98, 11623.
56. Becke, A. D. J Chem Phys 1993, 98, 5648.
57. Becke, A. D. J Chem Phys 1993, 98, 1372.
58. Becke, A. D. J Chem Phys 1997, 107, 8554.
59. Hamprecht, F. A.; Cohen, A. J.; Tozer, D. J.; Handy, N. C. J Chem Phys 1998, 109, 6264.
60. Wilson, P. J.; Bradley, T. J.; Tozer, D. J. J Chem Phys 2001, 115, 9233.
61. Schmider, H. L.; Becke, A. D. J Chem Phys 1998, 108, 9624.
62. Xu, X.; Goddard W. A., III. Proc Natl Acad Sci 2004, 101, 2673.
63. Adamo, C.; Cossi, M.; Barone, V. Theochem 1999, 493, 145.
64. Lynch, B. J.; Zhao, Y.; Truhlar, D. G. J Phys Chem A 2003, 107, 1384.
65. Zhao, Y.; Truhlar, D. G. J Phys Chem A 2004, 108, 6908.
66. Kormos, B. L.; Cramer, C. J. J Phys Org Chem 2002, 15, 712.
67. Lynch, B. J.; Fast, P. L.; Harris, M.; Truhlar, D. G. J Phys Chem A 2000, 104, 4811.
68. Becke, A. D. J Chem Phys 1996, 104, 1040.
69. Tao, J.; Perdew, J. P.; Staroverov, V. N.; Scuseria, G. E. Phys Rev Lett 2003, 91, 146401/146401.
70. Van Voorhis, T.; Scuseria, G. E. J Chem Phys 1998, 109, 400.
71. Zhao, Y.; Lynch, B. J.; Truhlar, D. G. J Phys Chem A 2004, 108, 2715.
72. Staroverov, V. N.; Scuseria, G. E.; Tao, J.; Perdew, J. P. J Chem Phys 2003, 119, 12129.
73. Krieger, J. B.; Chen, J.; Iafrate, G. J. Electron Correlations and Materials Properties, Plenum, New York, 1999; pp. 463.
74. Zhao, Y.; Truhlar, D. G. Phys Chem Chem Phys 2005, 7, 2701.
75. Boese, A. D.; Martin, J. M. L. J Chem Phys 2004, 121, 3405.
76. Quintal, M. M.; Karton, A.; Iron, M. A.; Boese, A. D.; Martin, J. M. L. J Phys Chem A 2006, 110, 709.
77. Gorelsky, S. I. SWizard Program, http://www.sg-chem.net/; Department of Chemistry, York University: Toronto, ON, 1998.
78. Pearl, G. M.; Zerner, M. C.; Broo, A.; McKelvey, J. J Comp Chem 1998, 19, 781.
79. Cowley, A. R.; Dilworth, J. R.; Donnelly, P. S.; Labisbal, E.; Sousa, A. J Am Chem Soc 2002, 124, 5270.
80. Blower, P. J.; Castle, T. C.; Cowley, A. R.; Dilworth, J. R.; Donnelly, P. S.; Labisbal, E.; Sowrey, F. E.; Teat, S. J.; Went, M. J. Dalton Trans 2003, 23, 4416.
81. Betts, H. M.; Barnard, P. J.; Bayly, S. R.; Dilworth, J. R.; Gee, A. D.; Holland, J. P. Angew Chem Int Ed 2008, 47, 8416.